Optics Letters

Multipass etalon cascade for high-resolution parallel spectroscopy

ANTONIO FIORE AND GIULIANO SCARCELLI*

Fischell Department of Bioengineering, University of Maryland, 8278 Paint Branch Drive, College Park, Maryland 20742, USA
**Corresponding author: scarc@umd.edu*

Received 18 December 2020; revised 12 January 2021; accepted 13 January 2021; posted 13 January 2021 (Doc. ID 418090); published 5 February 2021

Spectral contrast, the ability to measure frequency components of vastly different intensity, is critical in optical spectroscopy. For high spectral contrast at high spectral resolution, scanning etalons are generally used, as they allow cascading multiple dispersive elements. However, scanning instruments are inherently limited in terms of acquisition speed. Here we report a single-shot cascaded spectrometer design, in which light is dispersed along a single dispersion direction at every stage and thus can be recirculated in the same etalon multiple times. Using this design principle, we demonstrate single-shot spectral measurements at sub-gigahertz resolution and unprecedented spectral contrast (∼80 dB).

https://doi.org/10.1364/OL.418090

Optical spectroscopy is based on the spatial separation of light into its spectral components achieved by light dispersive elements in conjunction with a photon detector. A critical quality metric for spectral analysis and processing is the dynamic range, defined as the ability of the spectrometer to simultaneously measure signals, i.e., different frequencies, characterized by large difference in intensities. The dynamic range of a spectrometer is determined by the dynamic range of the photon detector and by the spectral contrast (also sometimes referred to as spectral extinction) of the dispersive process, i.e., the fraction of a spectral component incorrectly detected in neighboring spectral channels.

In the past, high spectral contrast has been accomplished by cascading multiple dispersive elements, as well as implementing multiple passes through the same dispersive element. However, since this approach is limited to the sampling of a single frequency, it requires integration into spectral scanning devices such as grating monochromators and Fabry–Perot scanning interferometers. Thus, the complete spectrum is obtained by sequential frequency scanning of single channels [1,2]. On the other hand, in instruments that can acquire an entire spectrum at once, also referred to as parallel or single-shot spectrometers, the cascade of dispersive elements has been achieved only in recent years in the so-called cross-axis configuration [3]. Such a configuration offers much higher speed in spectral acquisition, but it remains severely limited in scalability because of degradations of the instrumental linewidth which directly affects the spectral resolution. As a result, spectrometers with high spectral contrast are typically slow in spectral analysis and processing [4], while fast spectrometers have limited spectral contrast [5].

In this Letter, we present a novel approach to design spectrometers featuring a cascade of etalons which enables a high spectral contrast and rapid acquisition time without a significant compromise on the spectral resolution. Different from the previous cascading approach [4], in our design, light is dispersed on a single geometrical axis, allowing for iterative multipass implementation on a single etalon. We experimentally demonstrate an implementation of this novel spectrometer design using virtually imaged phased array (VIPA) etalons and performing Brillouin spectroscopy, an application where the weak inelastically scattered light component is extremely close ($\sim 0.01 - 0.001$ nm) to much stronger spectral components, typically back-reflections and elastically scattered light. We selected VIPA etalons because of the immediate impact of our innovation to the biological applications of Brillouin spectroscopy where spectral contrast and acquisition time are of critical importance. However, the same optical design concept of single-axis cascading could be extended to other dispersive elements such as diffraction gratings, echelle gratings, or prisms.

The working principle of single-axis parallel spectroscopy is shown in Fig. 1: when an input beam hits the first spectral dispersion element, it is spatially separated into its spectral components along a certain dispersion axis. This set of spectral components is spatially separated, and thus can be more easily filtered or analyzed. In a traditional spectrometer, each component is independently isolated and quantified using a single channel passing filter such as a slit; this allows for a high spectral contrast at the expense of measurement speed. In a parallel spectrometer, the components are instead sent to a

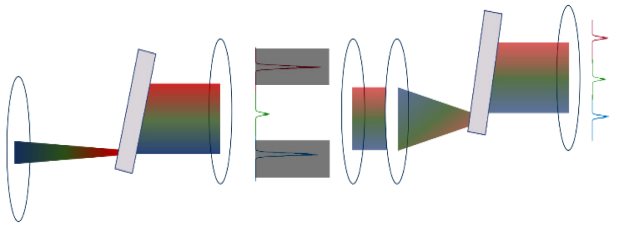

Fig. 1. Working principle of etalon cascade on a single axis. The red and blue components represent unwanted spectral components, filtered by the mask. The green component represents the signal frequency transmitted with optimized efficiency.

detector for the analysis of the whole spectrum. However, in experiments requiring high spectral contrast, the intensity of some of these components is so high that other components are not detectable, even using a high dynamic range sensor. Here we show that parallel spectral measurements are possible while filtering spectra as in scanning instruments by inserting suitable spectrum tailoring/filtering elements (such as masks, slits, or apodizing filters) that decrease the intensity of unwanted frequencies between dispersion stages [6–8]. The filtered spectrum is then reshuffled with a lens, and it enters a second spectral dispersive element, where it is further split into its spectral components along the same dispersion axis by the second stage of the spectrometer. In this way, the portion of the spectrum that is not rejected by the spatial filter (i.e., green component in Fig. 1) is propagated through the multiple stages, and only attenuated by the effective throughput of the dispersive elements. On the other hand, spectral components that need to be attenuated (red and blue components in Fig. 1) are reduced in intensity by the product of spectral extinction of the single dispersive elements and attenuation of the filtering elements. As the first stage in Fig. 1 reshuffles the light components into the second stage after the filtering element, the overall dispersive performances of the instrument are equivalent to the last stage, which operates as a single-shot spectral measurement, while the spectral contrast of the instrument are highly increased by the previous stages, which act as high efficiency customized bandpass filters.

The experimental setup is shown in Fig. 2. To demonstrate the main features of our novel method, we have built a three-stage cascaded parallel VIPA spectrometer using two VIPA etalons; in our design, the first two stages feature two passes in the same etalon via recirculation [9], while a third dispersive element is cascaded downstream. Light output from a single-mode fiber (SMF) is focused on the input window of a VIPA etalon which separates different spectral components at different angles; after the etalon, a cylindrical lens (CL) transforms the angular separation into a spatial separation at its focal plane. Unwanted spectral components are then rejected through a slit acting as a spatial filter. A set of lenses images the plane of the slit onto the VIPA1 entrance window on a different point to reduce crosstalk. Since the spectral components of the light are recombined through the focusing lens before the entrance into the VIPA etalon, the dispersive elements should be selected to optimize specifications. Here, to efficiently detect Brillouin scattered photons of biological media, typically in the frequency range between 7.5 and 8.5 GHz, we chose VIPA1 with a free spectral range (FSR) of 17 GHz. This maximizes the distance

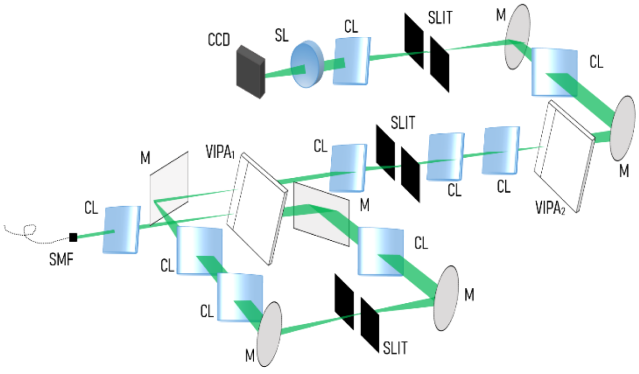

Fig. 2. Setup of a triple-pass single-axis VIPA spectrometer featuring two VIPA etalons.

between the Brillouin signal and elastically scattered photons, which represent the noise. In this way, cutting of the noise with the slit becomes straightforward. After the second dispersion, the light is filtered by a second spatial filter and subsequently focused into a second VIPA2 etalon, with an FSR of 20 GHz. Such a value for the final etalon is chosen to have the best resolution in measuring a range on frequencies in the biological field. Therefore, we provided an example of a three-stage spectrometer in which the first two stages are optimized for background cleanup, while the last one is optimized for spectral frequency measurement.

For optimal performances, two parameters need to be considered at each etalon stage. (1) The incident angle into the etalon determines the finesse, as shallower angles enable a larger number of interference sources, but too shallow of an angle can clip the beam and decrease throughput. A typical compromise of these two quantities usually stands around 35 finesse and 75% throughput. (2) The numerical aperture into the etalon determines the range of angles inserted into the VIPA and thus how many diffraction orders are observed in the output. Usually, to maximize throughput, only one or two orders are desired.

Next, we analyze the performances of this experimental arrangement. At first, we evaluated the spectral extinction of the instrument. The measurement of such quantity involves the separate evaluation of the filtering stages and the dispersive ones. The contrast of the two filtering stages was measured using a power meter, resulting in 57 dB of rejection. For this measurement, the filtering slit was engaged, blocking the unwanted signal as in a realistic measuring scenario. The dispersive stage spectral contrast was recorded with multiple spectral acquisitions at different exposure times to compensate for the limited dynamic range of the EMCCD camera [3]. The overall extinction resulted to be ∼79 dB. This value is ∼20 dB higher than double-stage spectrometers, but slightly under the theoretical maximum extinction of 90 dB, which we ascribe to the imperfect coupling of light into the VIPA2 etalon due to reduction in beam quality from stage to stage. Importantly, this extinction value can be further improved with apodized etalons [8,10].

In terms of throughput, single-axis cascading resulted in ∼10% overall throughput, which is better than previously reported cross-axis cascading methods [4]. Additionally, in terms of spectral resolution, this single-axis configuration is superior to cross-axis approaches. Since the same dispersion element can be used in both configurations, the ultimate performance will depend on the degradation of the single-stage instrumental linewidth. Cross-axis instruments have been shown to progressively distort the instrumental linewidth by a factor that depends on the rotation angle, with a reported spectral resolution of 0.6 GHz for two-stage instruments [10], and 0.7 GHz for three stages configurations [4]. In our case, we measured a spectral resolution of ∼0.52 GHz after three stages, demonstrating a significant improvement in instrumental linewidth degradation, comparable to single etalon performance. Such a result is a direct consequence of the dispersion followed by spectrum reshuffling between every cascading stage. In other words, the overall instrument provides the resolution of a single etalon approach (the last one in the cascade), while carrying the spectral extinction of three dispersive stages.

Subsequently, we built a confocal microscope linked to the spectrometer via the SMF in order to characterize the performances of the spectrometer for Brillouin light scattering

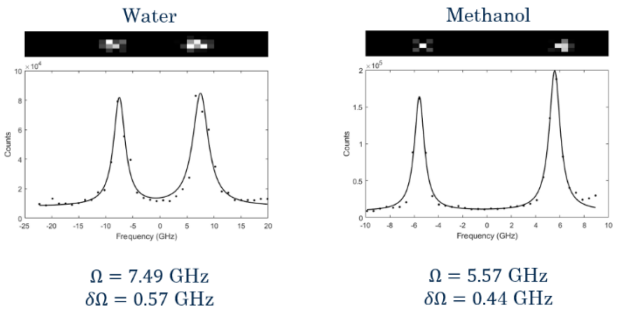

Fig. 3. Single frames and averaged spectra (frames $N = 20$) for two reference materials. The power used was 20 mW, with 1 s exposure time for water and 0.5 s for methanol. The measured Brillouin linewidth was 0.57 GHz for water and 0.44 GHz for methanol.

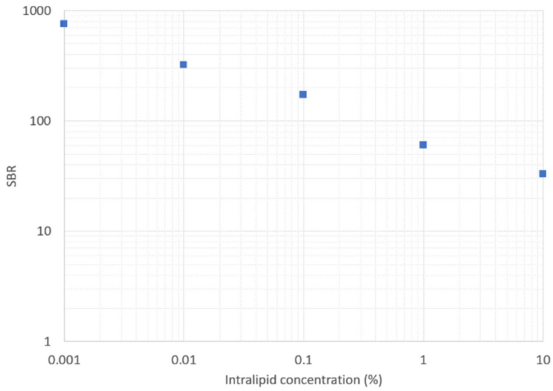

Fig. 4. Signal-to-background ratio performance of a triple-pass single-axis VIPA spectrometer in intralipid solutions.

spectroscopy. We measured the Brillouin spectra of water and methanol (Fig. 3). Since water and methanol have known Brillouin spectra, we also used these measurements to calibrate the spectrometer and verify its FSR; we obtained an FSR of 19.7 GHz, as expected, matching the manufactrurer's specifications of VIPA2.

To characterize the extinction properties of the spectrometer, we used intralipid tissue phantoms and measured the instrument signal to a background ratio (Fig. 4). As the sample becomes more turbid, the elastic scattering background is expected to increase making the Brillouin measurement noisier. We were able to perform a measurement at 10% intralipid concentration, which is representative of standard biological tissue [11–13] and obtained a signal to background ratio (SBR) greater than 10. Such an improvement when compared to instruments with a three-etalon pass [4] could be explained by the higher rejection of elastically scattered photons at given throughput, as well as better preservation of linewidth and higher throughput.

Next, we quantified the parallel spectral bandwidth of the single-axis cascade spectrometer. By the parallel spectral bandwidth, here we define the range of spectral components that are measured/processed simultaneously by the spectrometer. To place this quantity into context, a parallel spectrometer has a large parallel spectral bandwidth, usually given by the FSR of the dispersive element, and thus has a multiplexing factor equal to the finesse of the spectrometer (FSR/instrumental linewidth), typically above 30. In contrast, scanning spectrometers have a parallel spectral bandwidth equal to the instrumental linewidth

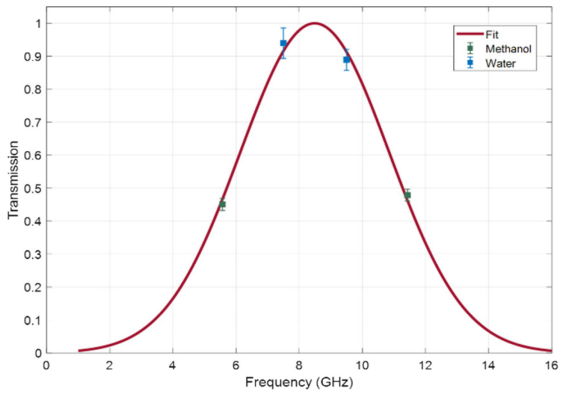

Fig. 5. Setup of a triple-pass single-axis VIPA spectrometer featuring two VIPA etalons. The water and methanol are used to fit a bandpass efficiency. The transmission of the water signal results in $T = 0.9$.

of the spectrometer, because they only transmit one spectral component at the time, i.e., a multiplexing factor of 1. Our scenario lies between these two extremes: the parallel spectral bandwidth is less than etalon FSR, because it is also affected by the aperture of the filtering slit and by the coupling of the beam focused into the VIPA etalons. We experimentally quantified our parallel spectral bandwidth using water and methanol Brillouin spectra. The water–methanol relative intensity of the signal was calibrated on a conventional cross-axis VIPA spectrometer [14], resulting in approximately 1:3. Knowing the relative scattering intensity of the two materials, we could characterize the overall spectral attenuation due to the convolution of all contributing factors. The resulting curve (Fig. 5) shows a bandwidth FWHM of 5.56 GHz. Considering the measured instrumental linewidth of 0.52 GHz, this yields a multiplexing factor of ∼10. Importantly, this multiplexity is more than enough to perform parallel high-resolution Brillouin spectroscopy, as it is close to the limit imposed by the Stokes and anti-Stokes signals of positive and negative spectral shifts.

In summary, the spectrometer described here offers a design alternative to multipass scanning etalons and parallel cross-axis cascades. Starting from this configuration, spectral performances can be further improved using previously demonstrated solutions such as apodization [6], interferometers [8], coronagraphy [7], and atomic absorption filters [15]. The performance demonstrated here has been obtained by using a filtering slit to cut the dominant and unwanted spectral lines, i.e., elastic scattering components, while letting the rest of the FSR through.

One critical design issue when considering single-axis cascading of multiple VIPA etalons is the matching of angles and numerical apertures at subsequent stages. In single etalon scenarios, or in two-stage cross-axis configurations, a Gaussian collimated beam is used to input the etalon, which can be optimally adjusted as previously described. Instead, here the VIPA pattern from a previous stage is the input into the entrance window of the next stage; this requires adjusting the input numerical aperture via sets of lenses and as a result the incident angle. We achieved a satisfactory operation point in this respect that is scalable to multiple stages as shown by the minimal linewidth degradation compared to the single stage and the superior throughput to three-stage cross-axis configuration; however, the matching remains suboptimal compared to Gaussian beam operation, which results in the excess insertion loss.

In conclusion, we have shown a novel spectroscopy approach using the same dispersion axis in a cascade configuration. This results in a high-resolution etalon spectrometer with extinction performances close to scanning instrument and acquisition times close to parallel spectroscopy.

Funding. National Science Foundation (1929412, 1942003); National Institutes of Health (R01EY028666, R01HD095520).

Disclosures. The authors declare no conflicts of interest.

REFERENCES

1. P. Hariharan and D. Sen, J. Opt. Soc. Am. **51**, 398 (1961).
2. J. R. Sandercock, Opt. Commun. **2**, 73 (1970).
3. G. Scarcelli, P. Kim, and S. H. Yun, Opt. Lett. **33**, 2979 (2008).
4. G. Scarcelli and S. H. Yun, Opt. Express **19**, 10913 (2011).
5. F. Scarponi, S. Mattana, S. Corezzi, S. Caponi, L. Comez, P. Sassi, A. Morresi, M. Paolantoni, L. Urbanelli, C. Emiliani, L. Roscini, L. Corte, G. Cardinali, F. Palombo, J. R. Sandercock, and D. Fioretto, Phys. Rev. X **7**, 031015 (2017).
6. G. Scarcelli and S. H. Yun, Nat. Photonics **2**, 39 (2008).
7. E. Edrei, M. C. Gather, and G. Scarcelli, Opt. Express **25**, 6895 (2017).
8. G. Antonacci, V. de Turris, A. Rosa, and G. Ruocco, Commun. Biol. **1**, 139 (2018).
9. A. Fiore and G. Scarcelli, Biomed. Opt. Express **10**, 1475 (2019).
10. G. Scarcelli, W. J. Polacheck, H. T. Nia, K. Patel, A. J. Grodzinsky, R. D. Kamm, and S. H. Yun, Nat. Methods **12**, 1132 (2015).
11. A. Fiore, J. Zhang, P. Shao, S. H. Yun, and G. Scarcelli, Appl. Phys. Lett. **108**, 203701 (2016).
12. S. Mattana, S. Caponi, F. Tamagnini, D. Fioretto, and F. Palombo, J. Innov. Opt. Health Sci. **10**, 1742001 (2017).
13. G. Antonacci, R. M. Pedrigi, A. Kondiboyina, V. V. Mehta, R. De Silva, C. Paterson, R. Krams, and P. Török, J. R. Soc. Interface **12**, 20150843 (2015).
14. K. V. Berghaus, S. H. Yun, and G. Scarcelli, J. Vis. Exp., **106**53468 (2015).
15. M. Zhaokai, A. J. Traverso, and V. Yakovlev, Opt. Express **22**, 5410 (2014).